

1 Article

2 **Mapping whole-event drive losses: the impact of race**
3 **profile and rider input on transmission efficiency in**
4 **cycling**

5 **George C Barnaby***, **Stuart Burgess** and **Jason Yon**

6 Department of Mechanical Engineering, Queen's Building, University of Bristol. BS8 1TR. UK
7

* Correspondence: (GB) george.barnaby@bristol.ac.uk

Received: date; Accepted: date; Published: date

8
9 **Abstract:** Several studies have considered the factors influencing transmission efficiency in a
10 bicycle. These conclude that the number of teeth in sprockets which are engaged with the chain
11 and the torque and cadence of the cyclist influence the frictional losses associated with
12 transmission between rider and rear wheel. These parameters may vary significantly during a
13 bicycle race since a rider modifies gear, power, and cadence to maximise physiological efficiency
14 for optimum bicycle velocity. Furthermore, gearing selection and power input varies between
15 riders, riding group and course profile. However, power models used to estimate race outcomes
16 tend to simplify efficiency to a single, arbitrary factor, describing losses which scale linearly with
17 input power regardless of expected regime. This study extends existing analytical descriptions
18 of transmission losses to the context of a road bicycle with front and rear derailleurs. The
19 calculated efficiency is considered within a cycling model to judge different regimes under
20 which the chain will typically operate and maps overall performance during an event. Efficiency
21 may vary significantly under certain loading regimes shown. In the context of highly trained
22 cyclists these differences result in small, linearly varying changes about a mean value. This
23 study shows there is limited error in assuming constant efficiency for certain race types, though
24 the efficiency value itself is dependent on several factors affecting the average loading regime.
25 Elevation profile of the racecourse and average power input from the rider are key parameters
26 affecting average efficiency. More massive riders racing at high average power input will
27 experience higher efficiency, while efficiency is higher across all riders racing courses with
28 increased elevation gain.

29 **Keywords:** transmission; efficiency; model; losses; bicycle; derailleur.

30
31 **1. Introduction**

32 In cycling, the use of analytical models
33 to describe the balance of input power at the
34 crank and output power at the tyre-road
35 interface allows the engineer to identify areas
36 for improvement in rider technique or
37 equipment design. One such model is
38 described in equation (1), based on an
39 analytical model from Martin et al, 1998.

$$P_{in} = V(F_a + F_r + F_g)/\eta, \quad \text{Eq. (1)}$$

40 where P_{in} is the input power of the rider; F_a ,
41 F_r and F_g are the resistive forces associated
42 with aerodynamic drag, rolling resistance
43 between tyre and road, and gravitational
44 resistance; V is the bicycle velocity; and η is
45 the transmission efficiency.

46 In deriving this model, and commonly
47 in literature, transmission efficiency is
48 assumed to be a constant value such that
49 losses scale linearly with power input, and
50 often an arbitrary estimate. Later studies,
51 however, demonstrate that the same chain in
52 a derailleur transmission system has



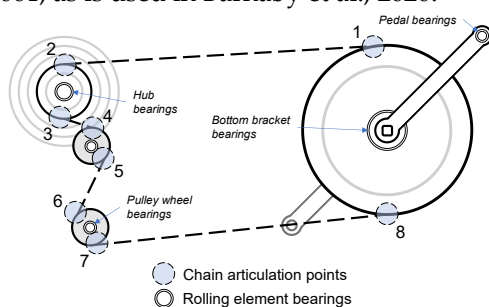
53 measured efficiency in the range 80.9 – 98.6%
 54 (Spicer et al., 2001). The changing factors
 55 causing this range in efficiency are input
 56 power, rotational speed, and gear
 57 configuration, which may also vary greatly
 58 during a bicycle race: gear shifts and non-
 59 consistent physiological output from the
 60 rider are common consequences of varying
 61 road-race profiles.

62 There is a gap in published literature for
 63 a holistic consideration of the efficiency to
 64 study these dependencies in the context of
 65 different racecourses and riders, which may
 66 be useful in determining the error in
 67 assuming constant efficiency and providing
 68 recommendations for what efficiency
 69 estimate to use for riders and engineers based
 70 on course and rider profile.

71 This study seeks to investigate the
 72 variability of transmission efficiency in
 73 expected regimes and defines the key factors
 74 influencing the transmission efficiency in
 75 usable terms, such that riders and engineers
 76 might be better informed in their use of an
 77 estimated efficiency in future modelling.

78 2. Frictional loss model

79 The authors are unaware of a
 80 comprehensive model of frictional losses in a
 81 bicycle derailleur drive in literature, and so
 82 have derived an analytical approach. This is
 83 an extension of the work of Lodge & Burgess,
 84 2001, as is used in Barnaby et al., 2020.



85

86 **Figure 1.** Sources of friction in a bicycle
 87 transmission, including rolling element
 88 bearings and points of chain articulation
 89 (numbered).

90 To determine the relative contribution of
 91 different sources of friction, Lodge &
 92 Burgess's analysis is used in conjunction with
 93 the geometry and spring rate of the rear
 94 derailleur to predict bottom-span tension,

95 and an industrial model of bearing losses is
 96 used to estimate friction in bearings (The SKF
 97 model for calculating the frictional moment).

98 The relative losses of each of the sources
 99 of friction, shown in Figure 1, is summarised
 100 in Table 1. There is significant contribution to
 101 losses of the high-tension span articulations
 102 (71%), reduced contribution from low-
 103 tension span articulations (24%), and a near-
 104 negligible contribution from rolling element
 105 bearings (3%). Friction in rolling element
 106 bearings is henceforth neglected in this
 107 analysis.

108 **Table 1.** Power losses are approximated for
 109 different sources of friction in the drive
 110 (300W / 90rpm)

	Power loss [W]	% of total
High-tension span ¹	5.5	71
Low-tension span ²	2.0	26
Rolling element bearings ³	0.2	3
Total	7.7	100

111 ¹ Chain links 1-2; ² Chain links 3-8; ³ pulley
 112 wheels, bottom bracket, rear hub, pedals

113 Transmission efficiency is defined as in
 114 equation 2:

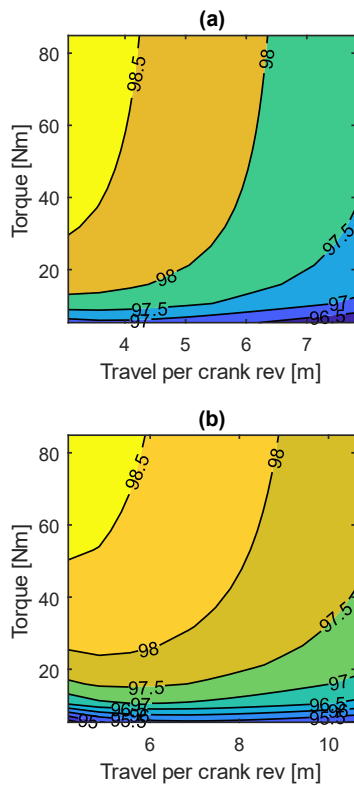
$$\eta = (P_{in} - N_s \omega_s \sum_{i=1}^8 W_i) / P_{in} \quad \text{Eq. (2)}$$

115 where W is the work done against friction in
 116 each of 8 articulating links (entry and exit to
 117 each sprocket), ω_s is the rotational frequency
 118 of the chainring (s^{-1}) and N_s is number of teeth
 119 in the chainring. Work done against friction
 120 is a function of chain geometry, articulation
 121 angle and chain tension, all of which may be
 122 calculated based on specific equipment and
 123 rider input. A further dependency is on
 124 coefficient of sliding friction within the chain
 125 links, which can be accurately determined
 126 experimentally using techniques such as
 127 those proposed by Wragge-Morley et al.,
 128 2017. The calculation for work done against
 129 friction is included in Appendix I.

130 2.1 Transmission efficiency variation

131 The variation of transmission efficiency
 132 is examined over a range of cycling torque
 133 inputs and riding gears, shown in Figure 2.
 134 The low, hill climbing gears offer higher

135 efficiency due to the reduced articulation
 136 angle. Positive correlation between input
 137 torque at the crank and efficiency is due to
 138 the relative reduction of significance of the
 139 bottom-span losses, which are independent
 140 of torque input. At low torque the torque-
 141 independent losses in the bottom-span,
 142 tensioned by the derailleur arm, are
 143 relatively more significant and so
 144 transmission efficiency changes rapidly as a
 145 function of torque.



146
 147 **Figure 2.** Power efficiency [%] contour map
 148 for varying rider torque and gear for 11-28
 149 tooth cassette sprockets engaged with (a) 39-
 150 tooth chainring; and (b) 53-tooth chainring.

151 3. Variable efficiency within power model

152 To model how transmission efficiency
 153 varies in a race, simulation of typical power
 154 input and race profile is necessary since
 155 efficiency depends on power and gear
 156 selection, themselves having multivariant
 157 dependencies. The power required to
 158 overcome resistance at steady speed cycling
 159 is given in equations (3) – (6), based on work
 160 by Martin et al., 1998.

$$P_{in} = (P_a + P_r + P_g)/\eta, \quad \text{Eq. (3)}$$

161 where power to overcome aerodynamic
 162 drag, P_a , is described in equation (4), power
 163 to overcome rolling resistance of the tyres, P_r ,
 164 is described in equation (5) and power to
 165 overcome gradient, P_g is described in
 166 equation (6).

$$P_a = 0.5\rho C_d A_f V^3, \quad \text{Eq. (4)}$$

167 where ρ is air density, C_d is coefficient of
 168 aerodynamic drag, A_f is the frontal area of
 169 bicycle and rider, and V is bicycle velocity.
 170 Note that wind velocity is assumed to be zero
 171 in this analysis.

$$P_r = mg C_{rr} V, \quad \text{Eq. (5)}$$

172 where m is total mass of rider and bicycle, g
 173 is the gravitational acceleration constant and
 174 C_{rr} is the coefficient of rolling friction
 175 between tyre and road surface. Upright,
 176 straight-line cycling is considered for this
 177 analysis.

$$P_g = mg \sin(\theta) V, \quad \text{Eq. (6)}$$

178 where θ is the angle of gradient. Typical
 179 values for variables shown in equations (4) –
 180 (6) are from Wilson, Papadopoulos, and
 181 Whitt, 2004.

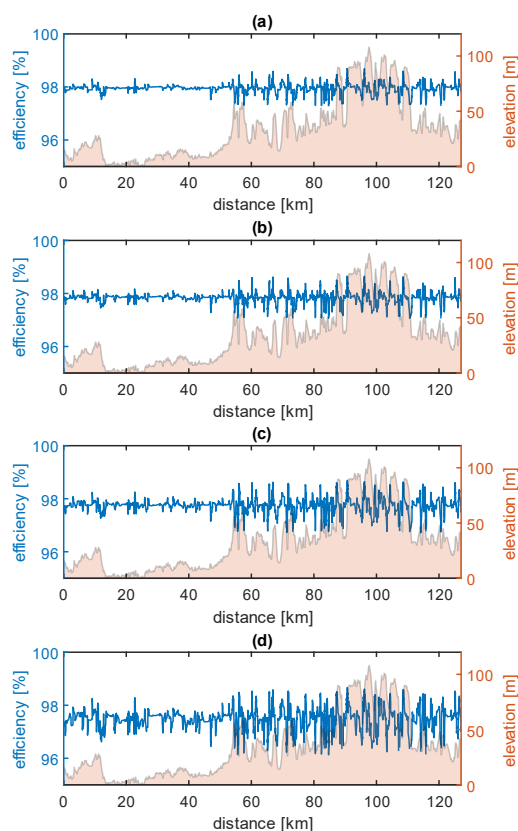
182 Steady-state velocity is calculated at
 183 many discrete points along a simulated
 184 racecourse for a typical bicycle drivetrain.

185 Gearing is selected to maintain cadence
 186 within a typical range, with chosen gearing
 187 influencing the calculation for efficiency
 188 according to the described frictional loss
 189 model. Further, a variable power input is
 190 applied such that power increases with
 191 positive gradient and decreases with
 192 negative gradient, shown to be an effective
 193 pacing strategy (Wells & Marwood, 2016).

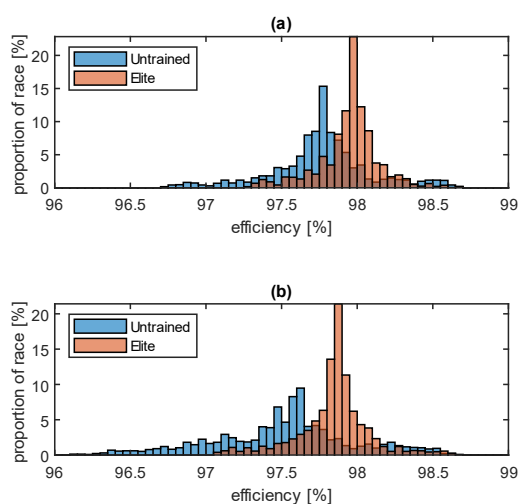
194 3.1 Efficiency variation by rider type

195 Transmission efficiency during an
 196 example elite race (part of the UCI 2021
 197 World Road Championships road-race from
 198 Antwerp to Leuven) is simulated and
 199 illustrated for four different riders in Figure
 200 3, where input parameters are summarised in
 201 Table 2. The spread of efficiency estimates

202 during simulated race for each case may be
203 seen in histograms in Figure 4.



204
205 **Figure 3.** Transmission efficiency
206 overlaid on Leuven 2021 road-race
207 course profile for a (a) elite male cyclist,
208 (b) elite female cyclist, (c) untrained
209 male cyclist, and (d) untrained female
210 cyclist.



211
212 **Figure 4.** Histogram of simulated
213 transmission efficiency during example race
214 for elite and untrained riders.

215 Efficiency can be seen to fluctuate with
216 the gradient of the course due to the changing
217 gear and power. Hill climbing gears and a
218 marginal increase in power both result in
219 increased efficiency as has been shown
220 previously. The opposite is true for negative
221 gradients, where smaller sprocket is engaged
222 and power is slightly reduced, decreasing
223 efficiency.

224 **Table 2.** Input parameters for four modelled
225 cases, with estimates for elite and untrained
226 male and female riders.

	Elite		Untrained	
	Male	Female	Male	Female
Mass [kg]	70	60	80	65
CdA [m ²]	0.3	0.25	0.4	0.3
Average power [W]	350	250	150	100
Cadence [rpm]	90±1 0	90±1 0	70±1 5	70±1 5
Average efficiency (S.D.) [%]	98.0 (0.20)	97.9 (0.24)	97.8 (0.33)	97.6 (0.46)

227 Comparing the proficient and untrained
228 cases, a larger variance can be seen in the
229 untrained cyclist as well as a slightly lower
230 average efficiency. This is illustrated more
231 clearly in Figure 4. The lower average
232 efficiency is largely due to the reduced power
233 input, and hence lower average torque. The
234 variance is reduced in the trained cyclist due
235 to the responsive gear changes working to
236 maintain a high cadence.

237 3.2 Efficiency variation in elite riders

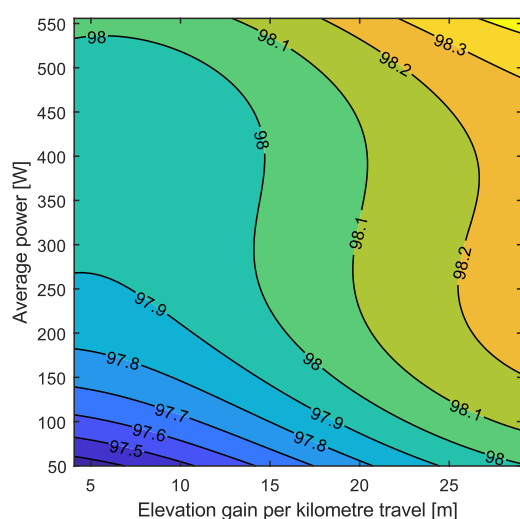
238 In elite level racing, efficiency variance
239 during a race is low and there is little error in
240 determining average velocity, or time to
241 completion, by using a single value efficiency
242 across an entire race. This is determined in
243 simulated races by finding the ratio of total
244 energy input and total energy output, found
245 by integrating the power output and input
246 with respect to time as in equation 7.

$$\eta = \frac{\int P_{in} - P_{lost} dt}{\int P_{in} dt}, \quad \text{Eq. (7)}$$

247 However, there is still dependency of
248 this average efficiency on power input and

249 gearing, which itself is dictated by the
250 elevation profile of a racecourse.

251 An effective average efficiency is
252 determined numerically by simulating racing
253 across 20 different grand tour events with
254 riders of varying input power (50-550W) and
255 mass (50-80kg). Dependency of average
256 efficiency on the climbing during the race
257 (measured as average metres elevation gain
258 per kilometre travel), and the average power
259 achieved by the rider during the race is
260 illustrated in Figure 5. Mass is less impactful
261 and can be accounted for by applying an
262 additional 0.1% efficiency per 20kg above
263 65kg. These results are valid for riders with a
264 power-to-weight ratio of between 2 and 6
265 W/kg.



266
267 **Figure 5.** Contour map of transmission
268 power efficiency [%] as function of average
269 power during a race and its elevation profile.

270 4. Discussion

271 The range in efficiency found in
272 previous research is not realised in loading
273 regimes typical in elite racing. This is largely
274 because of the narrow cadence range and
275 high torque in elite racing which leads to
276 small and linearly varying changes in
277 transmission efficiency. Provided this is
278 maintained during a race, there is little error
279 in using a single factor for efficiency.

280 However, average power and elevation
281 profile are two factors which can vary greatly
282 in elite cycling between different event styles
283 and rider physiologies, leading to consistent

284 changes to efficiency across a race. A
285 mountainous tour stage will see higher
286 efficiency than one which is flat by up to
287 0.5%-pts, which may be even more extreme if
288 considering specific hill climbing events.
289 Rider power input also will influence
290 average efficiency, meaning that more
291 powerful male riders racing TT courses at
292 maximal effort may experience an average
293 transmission efficiency up to 0.8%-pts higher
294 than a less powerful rider during an
295 endurance event. Female elite riders will
296 inherently experience a reduced
297 transmission efficiency than male elite riders
298 due to applying less power at the crank.

299 5. Practical Applications.

300 Transmission efficiency may usually be
301 experimentally examined in limited and
302 specific loading regimes. This gives limited
303 insight given the dependencies of efficiency
304 which vary during a bicycle race. This study
305 demonstrates that further applying the
306 results of such tests to contextualise
307 efficiency within the expected loading
308 regimes based on rider and course type may
309 offer additional accuracy in determining an
310 effective average efficiency. This may be
311 applied to future analytical modelling for
312 evaluating equipment upgrades or
313 determining pacing strategies.

314 Future research to further examine
315 influences on transmission efficiency is
316 needed to confirm the theory presented here,
317 including extensive practical testing which
318 may offer experimental validation.

319 **Funding:** This research was funded by
320 Engineering and Physical Sciences Research
321 Council and Renold Chain.

322 **Conflicts of Interest:** The authors declare no
323 conflict of interest. The funders had no role in the
324 design of the study; in the collection, analyses, or
325 interpretation of data; in the writing of the
326 manuscript, or in the decision to publish the
327 results.

328 References

- 329 1. Barnaby, G. C., Yon, J., & Burgess, S. (2020).
330 Sprocket Size Optimisation for Derailleur
331 Racing Bicycles. *Journal of Science and
332 Cycling*, 9(2), 36.

- 333 2. Lodge, C. J., & Burgess, S. C. (2001). A model
 334 of the tension and transmission efficiency of
 335 a bush roller chain. Proceedings of the
 336 Institution of Mechanical Engineers, Part C:
 337 Journal of Mechanical Engineering
 338 Science, 216(4), 385-394.
- 339 3. Martin, J. C., Milliken, D. L., Cobb, J. E.,
 340 McFadden, K. L., & Coggan, A. R. (1998).
 341 Validation of a mathematical model for road
 342 cycling power. Journal of applied
 343 biomechanics, 14(3), 276-291.
- 344 4. Spicer, J. B., Richardson, C. J., Ehrlich, M. J.,
 345 Bernstein, J. R., Fukuda, M., & Terada, M.
 346 (2001). Effects of frictional loss on bicycle
 347 chain drive efficiency. J. Mech. Des., 123(4),
 348 598-605.
- 349 5. The SKF model for calculating the frictional
 350 moment (n.d.). Retrieved from
 351 [https://www.skf.com/binaries/pub12/Image](https://www.skf.com/binaries/pub12/Images/s/0901d1968065e9e7-The-SKF-model-for-calculating-the-frictional-moment_tcm_12-299767.pdf)
 352 [s/0901d1968065e9e7-The-SKF-model-for-](https://www.skf.com/binaries/pub12/Images/s/0901d1968065e9e7-The-SKF-model-for-calculating-the-frictional-moment_tcm_12-299767.pdf)
 353 [calculating-the-frictional-moment_tcm_12-](https://www.skf.com/binaries/pub12/Images/s/0901d1968065e9e7-The-SKF-model-for-calculating-the-frictional-moment_tcm_12-299767.pdf)
 354 [299767.pdf](https://www.skf.com/binaries/pub12/Images/s/0901d1968065e9e7-The-SKF-model-for-calculating-the-frictional-moment_tcm_12-299767.pdf)
- 355 6. Wells, M. S., & Marwood, S. (2016). Effects of
 356 power variation on cycle performance
 357 during simulated hilly time-trials. European
 358 journal of sport science, 16(8), 912-918.
- 359 7. Wilson, D. G., Papadopoulos, J., & Whitt, F.
 360 R. (2004). *Bicycling science* (3rd ed.). MIT
 361 press.
- 362 8. Wragge-Morley, R., Yon, J., Lock, R.,
 363 Alexander, B., & Burgess, S. (2018). A novel
 364 pendulum test for measuring roller chain
 365 efficiency. Measurement Science and
 366 Technology, 29(7), 075008.

368 Appendix I

369 Work done against friction in
 370 articulating chain links as derived by Lodge
 371 & Burgess, 2001, is summarised here. Eight
 372 articulations are considered, at entry to and
 373 exit from each engaged sprocket. The work

374 done in articulating these links
 375 simultaneously represents the energy lost for
 376 the drive advancing by one link, which may
 377 be multiplied by the chain speed in link pitch
 378 per second to determine the power lost here.

379 *Work done in articulating chain links*

380 Articulation of inner and outer links
 381 results in relative sliding of different surfaces
 382 between the pin and bushing. Since they
 383 must alternate, an average is taken of the two
 384 to define work done for one articulation:

$$385 \quad W = (W_{pin} + W_{bush})/2$$

386 where work done during pin articulation is
 387 described as below:

$$388 \quad W_{pin} = \frac{F_i}{\sqrt{1 + \mu^2}} \mu r_{bi} \alpha_i$$

389 and work done during bush articulation is:

$$390 \quad W_{bush} = \frac{\mu F_c r_{bi} [\cos \theta_{RA} - \cos(\theta_{RA} + \alpha_m)]}{\sqrt{1 + \mu^2} \sin(\theta_{RA} + \alpha_m)} + \frac{\mu F_c r_{bo} (1 - \cos \alpha_m)}{\sin(\theta_{RA} + \alpha_m)}$$

391 Lodge & Burgess, 2001 should be consulted
 392 for definitions of these terms. These are
 393 determined by the geometry of the chain
 394 components and sprocket, except for
 395 coefficient of friction, μ , which is determined
 396 using accurate measurements as described in
 397 Wragge-Morley et al., 2017.

399 *Chain tension force*

400 The contact force between each of 8
 401 articulating links is calculated. Top span
 402 contact force is from crank torque acting at
 403 chainring radius and acts at articulations
 404 onto the chainring and off the engaged
 405 cassette sprocket. Bottom span contact force
 406 is equal for all 6 remaining articulations and
 407 resolved from the spring rate of the rear
 408 derailleur tension arm and its geometry.